Progress In Electromagnetics Research M, Vol. 33, 31–44, 2013

LOW RCS METAMATERIAL ABSORBER AND EXTENDING BANDWIDTH BASED ON ELECTROMAGNETIC RESONANCES

Huanhuan Yang*, Xiangyu Cao, Jun Gao, Wenqiang Li, Zidong Yuan, and Kai Shang

Information and Navigation Institute of Air Force Engineering University, Xi'an, Shaanxi 710077, China

Abstract—A low radar cross section (RCS) metamaterial absorber (MMA) with an enhanced bandwidth is presented both numerically and experimentally. The MMA is realized by assembling three simple square loops in a three-layer structure according to the idea of separating electric and magnetic resonances. Different from one-layer MMA, the proposed MMA can effectively couple with the electric and magnetic components of the incident wave in different positions for fixed frequency, while, for different frequencies, it can trap the input power into different dielectric layers and absorb it in the lossy substrate. Experimental results indicate that the MMA exhibits a bandwidth of absorbance above 90% which is 4.25 times as that of one-layer MMA, and 10 dB RCS reduction is achieved over the range of 4.77–5.06 GHz. Moreover, the cell dimensions and total thickness of the MMA are only 0.17λ and 0.015λ, respectively. The low RCS properties of the MMA are insensitive to both polarization and incident angles.

1. INTRODUCTION

The design of resonant metamaterial absorber (MMA) with near unity absorption has attracted intense attention since Landy et al. [1] firstly demonstrated a perfect MMA composed solely of metallic elements and lossy dielectric spacer. The design idea of this MMA is to adjust the effective $\varepsilon(\omega)$ and $\mu(\omega)$ independently by varying the dimensions of electric resonant component and magnetic resonant

Received 1 August 2013, Accepted 11 September 2013, Scheduled 16 September 2013

* Corresponding author: Huanhuan Yang (jianye8901@126.com).

component in the unit cell so as to match the effective impedance of MMA to free space and achieve a large resonant dissipation in the meantime. Thus, wave transmission and reflection are minimized simultaneously, and absorption is maximized. Compared with conventional absorbers [2–4], this kind of MMAs exhibits some unprecedented advantages including the ultra-thin thickness, lossless surface, simple as well as light configuration and easily-extendable absorbing frequencies [5–10]. Such advantages of MMAs render them potential candidates for bolometers, stealth and detection of explosives. However, one of the major obstacles for the practical applications of MMAs lies in the narrow bandwidth strongly dependent on electromagnetic (EM) resonances [11–14]. Quite recently, many efforts have been made on MMAs to achieve wide-angle as well as polarization-insensitive absorption [15–22], multi-band absorption [23–29] and tunable absorption [30–32]. But there are few literatures on the research of increasing the bandwidth. Multi-cells of different dimension elements with appropriate geometrical parameters patterned in a co-planar are presented in [33–35] to extend the bandwidth. Nevertheless, the strong EM couplings between cells with different parameters usually lower the absorption. Another method to enhance the bandwidth is discussed in [36, 37] where MMAs at THz and GHz are simulated by stacking several metallic layers with different dimensions. [38] combines the afore-mentioned methods to extend the bandwidth at microwave frequencies. However, the cell dimensions of the proposed MMAs in [33–39] are often very large, specifically, they are larger than $\lambda/4$. In [40, 41], the bandwidth is also improved through some special designs. But it is hard to enhance the bandwidth further.

Moreover, the most promising application of MMAs is EM stealth. To the best of the authors' knowledge, the absorbing properties rather than the radar cross section (RCS) reduction performance of MMAs have been widely analyzed in most research. The study of RCS reduction characteristic of MMAs remains comparatively less [42]. And the relationship between RCS reduction and absorbing properties has not been discussed. Besides, most of the present literatures are aimed at extending the full width at half maximum (FWHM) bandwidth. In this work, a conclusion that MMAs should demonstrate absorption above 90% to meet the demands of EM stealth is conducted through the investigation of RCS and absorption. Then the bandwidth of absorption above 90% is effectively extended by stacking three simple square loops according to the idea of separation of electric and magnetic resonances. Fields distributions are investigated to gain insight into the working mechanism. It is shown that the proposed MMA not only can produce electric and magnetic resonances in

different positions for fixed frequency, but also can trap the input power into different dielectric layers and absorb it in the lossy substrate for different frequencies, which effectively minishes the EM couplings and consequently keeps the strong absorbing properties in a wide frequency range. In addition, regardless of its small cell size, about 0.17λ, and ultra-thin thickness, almost 0.015λ, this MMA shows polarization-independent RCS reduction performance for wide incident angles.

2. RCS AND ABSORBANCE

Reflectance and transmittance are defined as $R(\omega) = |S_{11}|^2$, $T(\omega) = |S_{21}|^2$, respectively. For MMA backed by continuous metallic plate ($T(\omega) = 0$), the absorbance is calculated by

$$A(\omega) = 1 - R(\omega) - T(\omega) = 1 - R(\omega) \tag{1}$$

Reflectance can also be expressed by

$$R = \frac{|E^r|^2}{|E^i|^2} \tag{2}$$

where E^i is the incident field and E^r the reflected field.

According to the definition, RCS is given by

$$\sigma = \lim_{d\to\infty} 4\pi d^2 \frac{|E^s|^2}{|E^i|^2} \tag{3}$$

where E^s is the scattered field and d the detecting distance. For monostatic RCS under normal incidence, $E^s = E^r$, so RCS can be rewritten by

$$\sigma = \lim_{d\to\infty} 4\pi d^2 (1 - A) \tag{4}$$

Thus the RCS reduction of MMA compared with a PEC plate with comparable dimensions can be obtained by

$$\Delta\sigma = -10\log(1 - A)\,\mathrm{dB} \tag{5}$$

From Equation (5), it can be deduced that RCS reduction speedily goes up with the increase of absorbance. If A is 50%, the RCS reduction is only 3 dB, while if A is 90%, RCS reduction reaches 10 dB. It is worth noting that the foregoing results are all obtained under ideal conditions. Consequently, it can be concluded that MMAs should demonstrate absorption above 90% to meet the demands in practical EM stealth.

3. DESIGN AND SIMULATION

As shown in Figure 1, the proposed MMA consists of three stacked lossy dielectric layers, with a square metallic loop imprinted at the top of each of them. And the whole structure is backed by a continuous metal plane to ensure zero transmission. The complete symmetry of the unit cell along the x- and y-direction ensures the insensitive absorbance for arbitrary polarizations of incident wave. Starting with arbitrary dimensions and considering a normally incident plane wave propagating as Figure 1 shows, a genetic algorithm is adopted to obtain the optimal parameters for maximum absorption near 5 GHz. For comparison, a one-layer MMA operating at the same center frequency, which is formed by removing the two-tier dielectric spacers with upper imprinted square loops of the proposed MMA, is also designed. The substrate used in the MMAs is FR-4 with thickness of $h_j = 0.3$ mm ($j = 1, 2, 3$) and complex dielectric constants of $\varepsilon_r = 4.4(1 + i0.02)$. The metal portions of the MMAs are modeled as lossy copper with electric conductivity $\sigma_{\text{copper}} = 5.8 \times 10^7$ S/m. The final dimensions of the proposed MMA and one-layer MMA are shown in Table 1.

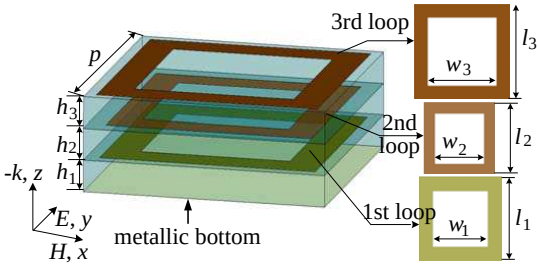

Figure 1. Schematic unit cell with dimensions of the proposed MMA.

Table 1. Dimensions of MMAs (all units in mm).

Sample	p	l_1	w_1	l_2	w_2	l_3	w_3
Proposed MMA	10.2	9.16	6.33	8.65	6.18	9.32	6.72
One-layer MMA	10.8	10.6	5.2	-	-	-	-

A full wave analysis provided by Ansoft HFSS has been carried out to investigate the EM properties of the MMA. Figure 2 shows the simulated absorbance as a function of frequency for different cases. As can be seen in Figure 2(a), the proposed MMA exhibits obvious near-unity absorbance at 4.81 GHz, 4.91 GHz and 5.01 GHz, respectively.

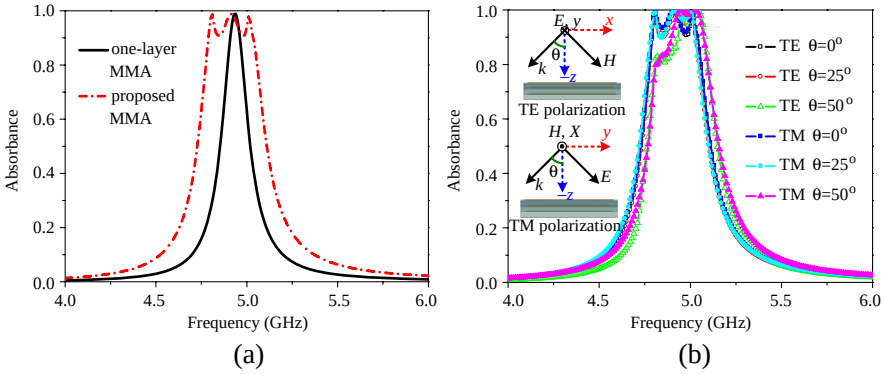

Figure 2. Simulated absorbing performance for (a) normal incidence, (b) different incident angles under TE and TM polarizations.

Table 2. Absorption bandwidth of MMAs.

Absorption bandwidth	One-layer MMA	Proposed MMA
FWHM	4.86–5.02 GHz (3.2%)	4.72–5.11 GHz (7.9%)
Absorbance above 90%	4.90–4.96 GHz (1.2%)	4.79–5.04 GHz (5.1%)

And the electric size of this MMA is only 0.17λ. Compared with the electric size of the MMA designed in [37], i.e., 0.4λ, the square loop pattern in the proposed MMA demonstrates good miniaturization effects. Table 2 clearly displays that the 90% absorption bandwidth of proposed MMA is 5.1%, which is much wider than that of one-layer MMA. The absorption under oblique incidence for TE and TM modes is plotted in Figure 2(b). As shown in the figure, the absorptive peaks remain greater than 80% with the incident angle ranging from 0° to 50° for TE mode. The similar conclusion can be drawn for TM mode. These results indicate that the proposed three-layer MMA is both polarization and incident angle insensitive.

To improve the physical understanding of the proposed MMA, we observed the electric field and current distributions at resonance frequencies. As can be seen in Figure 3(a), for one-layer MMA, charges accumulate mainly at the two ends of the square loop, indicating a response to the electric field component, while the currents are anti-parallel on the loop and ground, which induces a strong response to the magnetic field component. Numerical results for the proposed MMA are shown in Figure 3(b). For convenience, the square loops

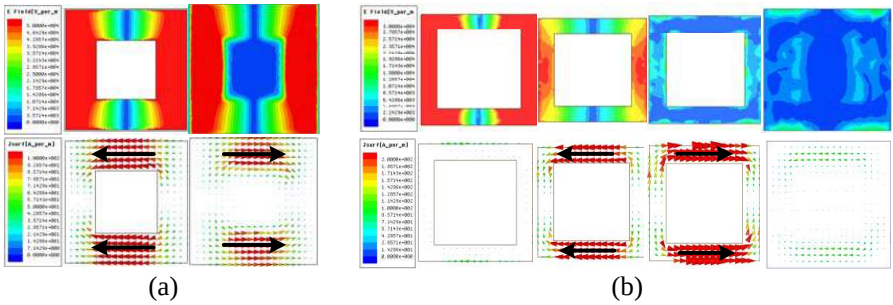

Figure 3. Electric fields and current distributions at 4.91 GHz of (a) one-layer MMA, (b) proposed MMA.

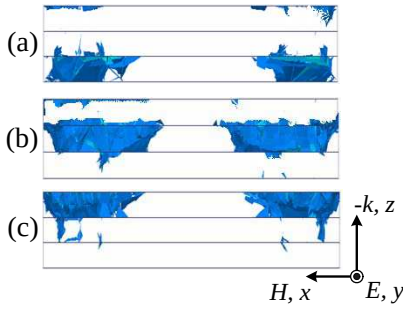

Figure 4. Distributions of power losses at strong absorptive frequencies. (a) 4.81 GHz, (b) 4.91 GHz, (c) 5.01 GHz.

in Figure 1 from the bottom to the top are denoted in sequence as 1st loop, 2nd loop and 3rd loop. As shown in Figure 3(b), 1st loop primarily couples with the electric field component, 2nd loop and 3rd loop response mostly to the magnetic field component. Thus electric and magnetic resonances can be observed in different layers at 4.91 GHz, which effectively reduces the mutual couplings. Owing to the strong EM couplings appearing at this frequency simultaneously, almost all of the incident power is trapped into the MMA. Taking a step further, Figure 4 displays the distributions of the power loss density at different peak absorption frequencies. It is clear to see that for the three strong absorptive frequencies, power losses are mainly associated with three different layers. As a result, the MMA exhibits three closely positioned absorption peaks.

Figure 5 shows the absorption for different material properties of metal layers and dielectric layers. The lossless metal (PEC) with lossy

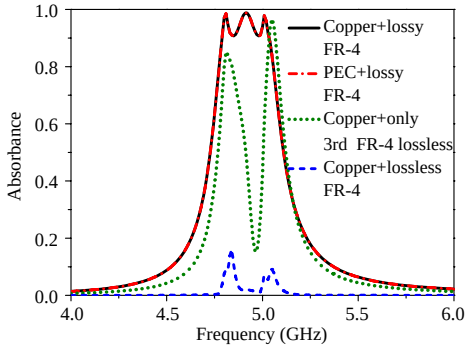

Figure 5. Absorption for different material properties of metal layers and dielectric layers.

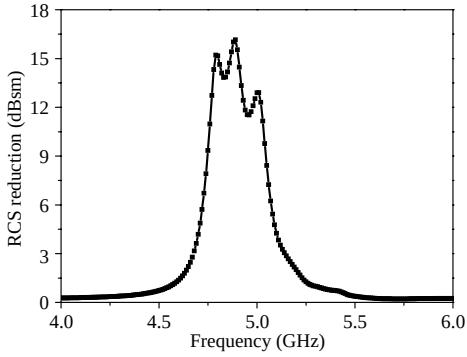

Figure 6. RCS reduction as a function of frequency under normal incidence.

FR-4 almost achieves perfect absorption of the copper with lossy FR-4. However, the copper with lossless FR-4 only achieves a maximum absorption of 16.1%. Therefore, it is concluded that the contribution to the strong absorption mainly comes from the dielectric losses in dielectric layers rather than the ohmic losses in metal [14]. To further confirm this point, we merely replaced the 3rd dielectric layer with lossless substrate and calculated the absorption. It is found that only the absorbance at 4.91 GHz drops dramatically, indicating that it is the 3rd dielectric layer that mostly results in the strong absorption at this frequency, which is in good accordance with the results shown in Figure 4(b).

The RCS properties of the MMA are studied by analyzing an absorbing board consisting of 10×10 proposed MMA array. The overall

size of the board is 102 mm × 102 mm. Monostatic RCS reduction of the board compared with those of a PEC plate with comparable dimensions is shown in Figure 6. As seen from the numerical results, the RCS reduction is above 10 dB from 4.75 GHz to 5.04 GHz for normal incidence. To stress the favorable absorbing properties of the board, we further compared the monostatic and bistatic RCS against the incident angles in Figure 7. It is observed that for monostatic case, the RCS of the board is below −18 dB with the incident angle ranging from −90° to 90°, and a prominent RCS reduction is almost obtained across the whole angle range. For bistatic RCS, a 10 dB reduction is achieved from −66° to 64°. These results suggest that the board exhibits low RCS properties in wide incident angles, which is also visually approved by observing the scattering fields shown in Figure 8.

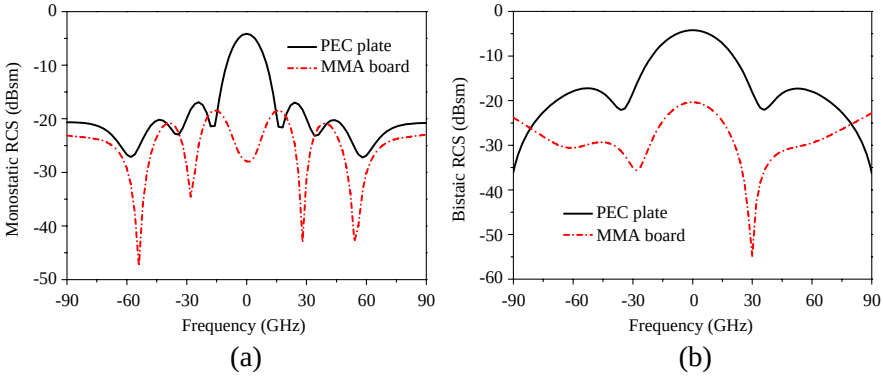

Figure 7. Comparison of RCS as a function of angles at 4.89 GHz. (a) Monostatic RCS, (b) bistatic RCS.

4. FABRICATION AND MEASUREMENT

First of all, we used the waveguide test system (closed system) [27] to verify the absorption. Each layer of the MMA sample composed of 2 × 3 unit cells was fabricated, as shown in the inset of Figure 9, based on printed circuit board (PCB) technology. Then they were spliced into the MMA sample. We connected a standard C-band waveguide BJ48 to Agilent N5230C network analyzer and mounted the sample into the port of the waveguide. As can be seen in Figure 9, the measured maximum absorbance is 98.7% at 4.81 GHz, and the absorbance exceeds 90% from 4.79 GHz to 5.03 GHz. Regardless of the slight frequency deviation caused by bonding layers, a good agreement

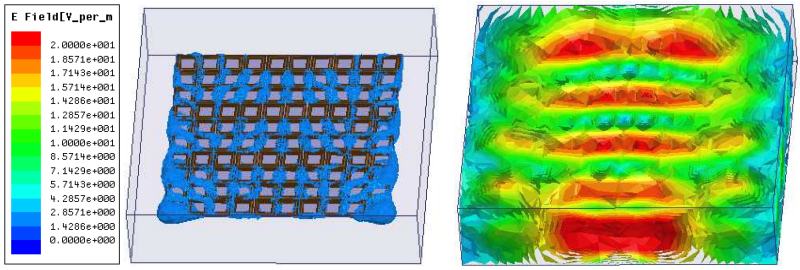

Figure 8. Distributions of scattering fields at 4.89 GHz of (a) proposed MMA board, (b) PEC plate.

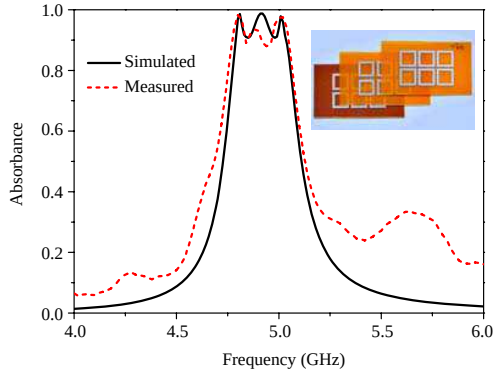

Figure 9. Comparison of simulated and measured absorption.

between simulated and measured results is obtained, which verifies the extended high absorption bandwidth of the proposed MMA.

The absorbing board consisting of 10×10 unit cells was also fabricated using PCB technology. Figure 10 shows the fabricated samples and the MMA board under testing. Monostatic RCS of the MMA sample and a PEC plate in the same size were measured in anechoic chamber. To ensure the accuracy of the measurements, the distance between the testing horn antennas and the sample is set to be 1 m. Figure 11 compares the measured results with simulated as well as calculated ones. The calculated results are obtained by putting the absorbance of proposed MMA in Figure 2(a) into Equation (5). We can see that an evident RCS reduction above 10 dB is obtained from 4.77 GHz to 5.06 GHz in measurements. The small error between simulated and measured results is due to the adherence deviations. In addition, the discrepancy of simulated and calculated results can

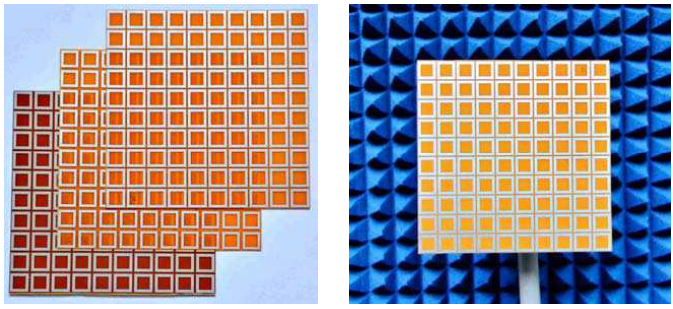

Figure 10. Photographs of (a) fabricated samples, (b) the MMA board under testing.

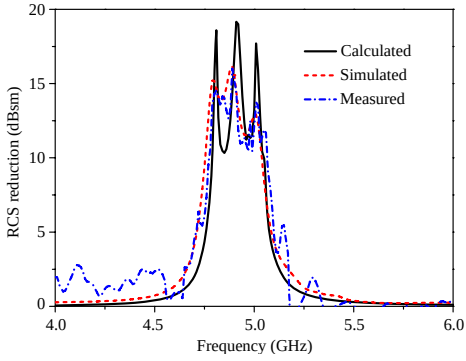

Figure 11. Comparison of calculated and simulated as well as measured RCS reduction.

be attributed to the factor that the size of the simulated model is 102 mm × 102 mm whereas the calculated results correspond to infinite size. Measured results once again prove the low RCS properties of proposed MMA.

5. CONCLUSION

A low-RCS metamaterial absorber (MMA) with enhanced bandwidth is designed and fabricated in this paper. The relationship between RCS reduction and absorbance of MMA is discussed first. Then according to the idea of separating the electric and magnetic resonances, the bandwidth of MMA is effectively extended by assembling three square loops with appropriate geometrical dimensions. Investigation into

fields distributions suggest that the proposed MMA not only can offer electric and magnetic couplings to the incident wave in different positions for fixed frequency, but also can trap the input power into different dielectric layers and absorb it in the lossy substrate for different frequencies. Owing to this property, the bandwidth of absorbance above 90% of the three-layer MMA is 4.25 times as that of one-layer MMA. About 10 dB RCS reduction is achieved over the range of 4.77–5.06 GHz in measurements. Considering the small dimensions of the unit cell, about 0.17λ, and the ultra-thin thickness of 0.015λ, we believe that the bandwidth of the MMA can be further broadened by increasing the number of stacked layers with the same or different cell configurations. Moreover, the proposed MMA may have strong practical and bright application foreground due to its advantages of simple design, easy fabrication, stable performance as well as enhanced bandwidth.

ACKNOWLEDGMENT

This work was supported by the National Natural Science Foundation of China (No. 61271100) and the Natural Science Foundation of Shaanxi province (No. 2010JZ010).

REFERENCES

1. Landy, N. I., S. Sajuyigbe, J. J. Mock, et al., "Perfect metamaterial absorber," *Physical Review Letters*, Vol. 100, 207402, 2008.
2. Fante, R. L. and M. T. McCormack, "Reflection properties of the Salisbury screen," *IEEE Trans. Antennas Propag.*, Vol. 36, No. 10, 1443–1454, 1988.
3. Chambers, B. and A. Tennant, "Optimised design of Jaumann radar absorbing materials using a genetic algorithm," *IEE Proc. — Radar, Sonar Navig.*, Vol. 143, No. 1, 23–30, 1996.
4. Reinert, J., J. Psilopoulos, J. Grubert, and A. Jacob, "On the potential of graded-chiral dallenbach absorbers," *Microwave and Optical Technology Letters*, Vol. 30, No. 4, 254–257, 2001.
5. Li, M., H.-L. Yang, X.-W. Hou, Y. Tian, and D.-Y. Hou, "Perfect metamaterial absorber with dual bands," *Progress In Electromagnetics Research*, Vol. 108, 37–49, 2010.
6. Hu, T., N. I. Landy, C. M. Bingham, et al., "A metamaterial absorber for the terahertz regime: Design, fabrication and characterization," *Optics Express*, Vol. 16, 7181–7188, 2008.

7. Zhang, F., L. Yang, Y. Jin, and S. He, "Turn a highly-reflective metal into an omnidirectional broadband absorber by coating a purely-dielectric thin layer of grating," *Progress In Electromagnetics Research*, Vol. 134, 95–109, 2013.
8. Dayal, G. and S. A. Ramakrishna, "Design of highly absorbing metamaterials for infrared frequencies," *Optics Express*, Vol. 20, 17503–17508, 2012.
9. Jiang, Z. H., S. Yun, F. Toor, et al., "Conformal dual-band near-perfectly absorbing mid-infrared metamaterial coating," *ACS Nano*, Vol. 5, 4641–4647, 2011.
10. Wang, J. Q., C. Z. Fan, P. Ding, et al., "Tunable broad-band perfect absorber by exciting of multiple plasmon resonances at optical frequency," *Optics Express*, Vol. 20, 14871–14878, 2012.
11. Hao, J., et al., "High performance optical absorber based on a plasmonic metamaterial," *Applied Physics Letters*, Vol. 96, No. 25, 251104, 2010.
12. Zhou, H., F. Ding, Y. Jin, and S. He, "Terahertz metamaterial modulators based on absorption," *Progress In Electromagnetics Research*, Vol. 119, 449–460, 2011.
13. He, X.-J., Y. Wang, J. Wang, T. Gui, and Q. Wu, "Dual-band terahertz metamaterial absorber with polarization insensitivity and wide incident angle," *Progress In Electromagnetics Research*, Vol. 115, 381–397, 2011.
14. Costa, F., et al., "A circuit-based model for the interpretation of perfect metamaterial absorber," *IEEE Trans. Antennas Propag.*, Vol. 61, No. 3, 1201–1209, 2013.
15. Hu, T., C. M. Bingham, A. C. Strikwerda, et al., "Highly flexible wide angle of incidence terhertz metamaterial absorber: Design, fabrication, and characterization," *Physical Review B*, Vol. 78, No. 24, 2411031–2411034, 2008.
16. Luukkonen, O., F. Costa, A. Monorchio, et al., "A thin electromagnetic absorber for wide incidence angles and both polarizations," *IEEE Trans. Antennas Propag.*, Vol. 57, No. 10, 3119–3125, 2009.
17. Landy, N. I., C. M. Bingham, T. Tyler, et al., "Design, theory, and measurement of a polarization-insensitive absorber for terahertz imaging," *Physical Review B*, Vol. 79, 125104, 2009.
18. Zhu, B., Z. Wang, C. Huang, Y. Feng, J. Zhao, and T. Jiang, "Polarization intsensitive metamaterial absorber with wide incident angle," *Progress In Electromagnetics Research*, Vol. 101, 231–239, 2010.

19. Grant, J., Y. Ma, S. Saha, et al., "Polarization insensitive terahertz metamaterial absorber," *Optics Letters*, Vol. 36, 1524–1526, 2011.
20. Aydin, K., V. E. Ferry, R. M. Briggs, and H. A. Atwater, "Broadband polarization-independent resonant light absorption using ultrathin plasmonic super absorbers," *Nature Communications*, Vol. 2, 517, 2011.
21. Lu, L., S. Qu, H. Ma, F. Yu, S. Xia, Z. Xu, and P. Bai, "A polarization-independent wide-angle dual directional absorption metamaterial absorber," *Progress In Electromagnetics Research M*, Vol. 27, 191–201, 2012.
22. Lee, J., Y. Yoon, and S. Lim, "Ultra-thin polarization independent absorber using hexagonal interdigital metamaterial," *ETRI Journal*, Vol. 34, No. 1, 126–129, 2012.
23. Hu, T., C. M. Bingham, D. Pilon, et al., "A dual band terahertz metamaterial absorber," *Journal of Physics D: Applied Physics*, Vol. 43, No. 22, 2251021–2251025, 2010.
24. Ma, Y., Q. Chen, J. Grant, et al., "A terahertz polarization insensitive dual band metamaterial absorber," *Optics Letters*, Vol. 36, No. 6, 945–947, 2011.
25. Furkan, D., K. Muharrem, U. Emin, and S. Cumali, "Dual-band polarization independent metamaterial absorber based on omega resonator and octa-starstrip configuration," *Progress In Electromagnetics Research*, Vol. 141, 219–231, 2013.
26. Li, H., L. Yuan, B. Zhou, et al., "Ultrathin multiband gigahertz metamaterial absorbers," *Journal of Applied Physics*, Vol. 110, No. 1, 0149091–0149098, 2011.
27. Li, L., Y. Yang, and C. Liang, "A wide-angle polarization-insensitive ultra-thin metamaterial absorber with three resonant modes," *Journal of Applied Physics*, Vol. 110, No. 6, 0637021–0637025, 2011.
28. Huang, L. and H. Chen, "Multi-band and polarization insensitive metamaterial absorber," *Progress In Electromagnetics Research*, Vol. 113, 103–110, 2011.
29. Shen, X., Y. Yang, Y. Zang, et al., "Triple-band terahertz metamaterial absorber: Design, experiment, and physical interpretation," *Applied Physics Letters*, Vol. 101, No. 15, 1541021–1541024, 2012.
30. Zhu, B., C. Huang, Y. Feng, J. Zhao, and T. Jiang, "Dual band switchable metamaterial electromagnetic absorber," *Progress In Electromagnetics Research B*, Vol. 24, 121–129, 2010.

31. Zhu, W., Y. Huang, I. Rukhlenko, et al., "Configurable metamaterial absorber with pseudo wideband spectrum," *Optics Express*, Vol. 20, No. 6, 6616–6621, 2012.
32. Shi, J. H., Z. Zhu, H. F. Ma, et al., "Tunable symmetric and asymmetric resonances in an asymmetrical splitring metamaterial," *Journal of Applied Physics*, Vol. 112, No. 7, 0735221–0735225, 2012.
33. Luo, H., Y. Z. Cheng, and R. Z. Gong, "Numerical study of metamaterial absorber and extending absorbance bandwidth based on multi-square patches," *European Physical Journal B*, Vol. 81, 387–392, 2011.
34. Luo, H., T. Wang, R. Gong, Y. Nie, and X. Wang, "Extending the bandwidth of electric ring resonator metamaterial absorber," *Chinese Phys. Lett.*, Vol. 28, No. 3, 034204, 2011.
35. Dimitriadis, A. I., et al., "A polarization-/angle-insensitive, bandwidth-optimized, metamaterial absorber in the microwave regime," *Appl. Phys. A — Mater.*, Vol. 109, No. 4, 1065–1070, 2012.
36. Ye, Y. Q., Y. Jin, and S. L. He, "Omni-directional, broadband and polarization-insensitive thin absorber in the terahertz regime," *Physics Optics*, Vol. 11, 1–6, 2009.
37. Ding, F., et al., "Ultra-broadband microwave metamaterial absorber," *Applied Physics Letters*, Vol. 100, 103506, 2012.
38. Bao, S., C. R. Luo, Y. P. Zhang, and X. P. Zhao, "Broadband metamaterial absorber based on dendritic structure," *Acta Phys. Sin.*, Vol. 59, No. 5, 318701–318705, 2010.
39. Sun, J., et al., "An extremely broad band metamaterial absorber based on destructive interference," *Optics Express*, Vol. 19, No. 22, 21155–21162, 2011.
40. Gu, C., S. Qu, Z. Pei, H. Zhou, J. Wang, B.-Q. Lin, Z. Xu, P. Bai, and W.-D. Peng, "A wide-band, polarization-insensitive and wide-angle terahertz metamaterial absorber," *Progress In Electromagnetics Research Letters*, Vol. 17, 171–179, 2010.
41. Lee, J. Y. and S. J. Lim, "Bandwidth-enhanced and polarisation-insensitive metamaterial absorber using double resonance," *Electronics Letters*, Vol. 47, No. 1, 8–9, 2011.
42. Culhaoglu, A. E., et al., "Mono- and bistatic scattering reduction by a metamaterial low reflection coating," *IEEE Trans. Antennas Propag.*, Vol. 61, No. 1, 462–466, 2013.